Strong Hall voltage modulation in hybrid ferromagnet/semiconductor microstructures

F. G. Monzon, Mark Johnson,[a] and M. L. Roukes[b]
Condensed Matter Physics 114-36, California Institute of Technology, Pasadena, California 91125

(Received 4 February 1997; accepted for publication 19 September 1997)

We present a new magnetoelectronic device consisting of a μm-scale semiconductor cross junction and a patterned, electrically isolated, ferromagnetic overlayer with in-plane magnetization. The large local magnetic field emanating from the edge of the thin ferromagnetic film has a strong perpendicular magnetic component, $B_\perp(\mathbf{r})$, which induces a Hall resistance, R_H, in the microjunction. External application of a weak in-plane magnetic field reverses the magnetization of the ferromagnet and with it $B_\perp(\mathbf{r})$, thus modulating R_H. Our data demonstrate that this strong ''local'' Hall effect is operative at both cryogenic and room temperatures, and is promising for device applications such as field sensors or integrated nonvolatile memory cells. © *1997 American Institute of Physics.* [S0003-6951(97)00747-X]

Novel magnetoelectronic devices form an area of current and growing interest. Examples of this relatively new area of research[1] are studies of giant magnetoresistance (GMR) structures,[2] spin-dependent tunneling devices,[3] and spin transistors.[4] These rely on both the spin of the current carriers and the relative magnetization of two or more ferromagnetic films to achieve modulation of electrical transport properties. Micromagnetic phenomena occurring in small ferromagnetic films are also of current interest, in part because they must be understood and optimized for the magnetoelectronic microdevice applications in which they play a crucial role. This optimization is necessary both to control domain structure and to minimize fringe fields that can induce extraneous magnetostatic coupling between ferromagnetic layers.

By contrast, in this letter we describe a novel hybrid ferromagnet/semiconductor structure whose operation is based upon the substantial fringe field, $\mathbf{B}(\mathbf{r})$, at the edge of a single, μm-scale, low-coercivity ferromagnetic film (F).[5] While these local fields are large, of order kOe near the edges of F, their polarity is readily switched by application of a much smaller in-plane field, $H_\parallel$ which reverses $\mathbf{M} = M\hat{x}$, the magnetization of F. Figure 1 illustrates the device geometry. The ferromagnetic film F is positioned a small distance, s, from the center of the cross junction [Fig. 1(a)]. In-plane magnetization $\mathbf{M}$ generates a local magnetic field, $\mathbf{B}(\mathbf{r})$, with a large local component *perpendicular* to the conducting layer, which changes sign with $\mathbf{M}$. In an ideal film this ''switching'' can occur for $H_\parallel$ of order tens of Oe. Reversal of $\mathbf{M}$ results in a bipolar swing of the Hall voltage, $V_H = IR_H$, where I is the sense current. The built-in R_H in our devices is greater than the Hall resistance that would be found in a simple semiconductor Hall cross exposed to a perpendicular field of the same magnitude as the parallel field, $H_\parallel$. We believe it can provide the basis for new classes of magnetoelectronic devices.

The cross junctions were fabricated by standard microfabrication techniques using a high mobility n-type GaAs 2DEG. At $T = 300$ K (4.2 K), the 2DEG, located about 77 nm below the heterostructure surface, had density $n_s = 2.3 \times 10^{11}$ cm^{-2} (1.5×10^{11}) and mobility $\mu = 8.4 \times 10^3$ cm^2/V s (1.1×10^6). After the junction patterning steps, a permalloy film layer was thermally deposited from a $Ni_{0.81}Fe_{0.19}$ source, then patterned by optical lithography and liftoff. During the deposition of F, a small magnetic field was applied in the sample plane to induce an easy axis of magnetization along $\hat{x}$ [Fig. 1(a)].

Conventional four-probe ac magnetotransport measurements were made on these devices using sense currents from 0.3 to 1 μA while an in-plane field, $H_\parallel$, was swept over roughly ± 400 Oe. Prior to each sweep, an in-plane field of 500 Oe was applied to saturate $\mathbf{M}$. Data for a typical device are shown in Fig. 2. At 4.2 K, the offset $R_{os} = 1/2[R_H(+M\hat{x}) + R_H(-M\hat{x})]$ (see below) is very small and $R_H(\mathbf{M})$, which is a function of $H_\parallel$, directly mirrors the hysteresis loop, $\mathbf{M}(H_\parallel)$, of F.

Two trends were seen in the data from all devices. First, the hysteresis loops contracted with increasing temperature. Separate measurements of $\mathbf{M}$ in larger, but otherwise identical films, indicate that this results from decreasing permalloy film coercivity with increasing temperature. Second, the overall magnitude of $R_H(\propto 1/n_s)$ generally decreased with increasing temperature [Fig. 3 (*inset*)]. We attribute this, in large part, to increases in n_s with increasing temperature as discussed below (see also Fig. 4). Consistent with this picture, the growth of the offset R_{os} at higher temperatures is in

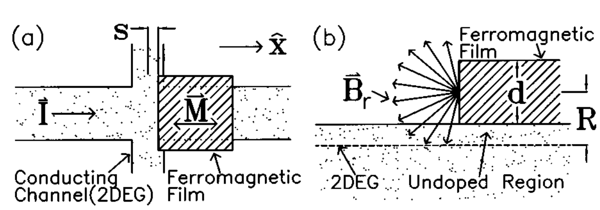

FIG. 1. Schematic diagram of: (a) the device geometry with 3×5 μm^2 cross junction and 7×7 μm^2 ferromagnetic film; and (b) a side view showing the radial magnetic field produced by a line of magnetic charge. The ferromagnetic film has thickness d, offset s, and has its midpoint a distance R above the 2DEG.

[a]Naval Research Laboratory 6341, Washington, DC 20375-5000.
[b]Electronic mail: roukes@caltech.edu

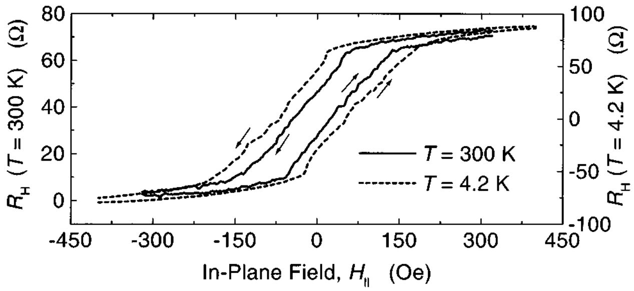

FIG. 2. Representative data for chip A devices at $T=4.2$ (dashed) and $T=300$ K (solid). The curves are hysteresis loops in which the local field from the ferromagnetic film induces a Hall voltage that mirrors the film magnetization.

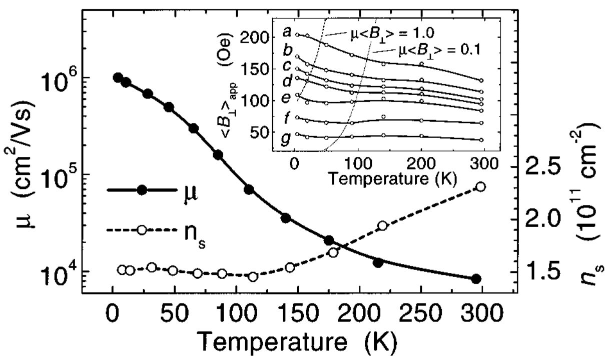

FIG. 4. Carrier density n_s and mobility μ vs temperature for the 2DEG used in these experiments (data from independent Hall bar measurements). *Inset*: Experimentally determined $\langle B_\perp \rangle_{\mathrm{app}}$, extracted from ΔR_H, for the same devices plotted in the inset of Fig. 3. The temperature-dependent density contribution has been divided out so that most of the variation occurs for lower temperatures, where ballistic phenomena occur.

direct proportion to the increasing 2DEG sheet resistance, $R_\square = 1/(n_s e \mu)$. The vertical offset at $T=300$ K (Fig. 2) is an effect arising from unintentional junction asymmetries: given that $R_\square(300\text{ K}) = 3200\ \Omega$, extremely careful control of the junction definition is required to obtain R_{os} less than a few ohms. With more precise lithography and etching (not our primary focus here), R_{os} could be engineered to take on virtually any desired value, e.g., to yield either a symmetric or a unipolar output characteristic.

In Fig. 3 we present the dependence of ΔR_H on relative magnet position s, obtained at $T=4.2$ K from ten devices on two separate chips (A and B, with five devices each), where s was measured by electron microscopy after fabrication. Both the peak in the ΔR_H data near $s=0$ and the rapid decrease of ΔR_H over a scale of about 1 μm validate the qualitative picture for $B_\perp(\mathbf{r})$ depicted in Fig. 1(b). The data point at $s=6.5\ \mu$m represents a control device: when the edge of F is removed from the vicinity of the Hall cross, there is no modulation of the Hall voltage.

To test our picture further, we estimate $B_\perp(\mathbf{r})$ considering F to be comprised of a single magnetic domain with $\mathbf{M} = M_s \hat{x}$. The resulting field can then be attributed to magnetic surface charge density M_s (magnetic ''charge'' per unit area) at the film's edge. In this simplest approximation, M_s is assumed to be concentrated along a line at the edge of F, a distance $d/2$ above the semiconductor surface [Fig. 1(b)], where d is the thickness of F. For an infinite line of magnetic charge density $\lambda_m = M_s d$ we obtain, in cylindrical coordinates, a radial field with magnitude $B_r(r) = 2\lambda_m / r$. The origin $r=0$ is defined along the line of charge, and fringe fields from the other edges of F are neglected, as justified by the results below. In the plane of the 2DEG, this yields $B_\perp(x) = 2\lambda_m R/(x^2+R^2)$, where x is the lateral distance between the edge of F and the point r, and R is the depth of the 2DEG relative to λ_m [Fig. 1(b)]. For chip A (B), we have $M_s \approx 838\ \mathrm{emu/cm^3}$ (838),[6] $d=150$ nm (105), and $R=152$ nm (130). This implies peak field values, directly beneath the edge of F (at $x=0$) of $B_\perp \approx 1650$ Oe (1350) falling to $B_\perp \approx 1150$ Oe (850) at $x=100$ nm and to only ≈ 37 Oe (22) at $x=1\ \mu$m.

In our novel devices, the field $B_\perp(x)$ has a steep gradient $\partial B_\perp / \partial x$ on the scale of the width w of the cross. To make a rough estimate of ΔR_H in this homogeneous field, we average $B_\perp(r)$ along x over a distance corresponding to the electrical width of our junctions, w (estimated to be $\approx 2.2\ \mu$m).[7] We then approximate the full bipolar swing upon magnetization reversal as $\Delta R_H \approx 2\langle B_\perp \rangle/(n_s e)$, where $\langle B_\perp \rangle$ is the averaged perpendicular field. Results for ΔR_H from this simple line charge model decay with increasing s much more quickly than shown by experiment. This suggests that the edges of our films were lithographically and/or magnetically rough. Despite our neglect of the steep field gradients and of the planar components of local fields, the predicted peak values for ΔR_H at $s=0$—269 Ω for chip A and 191 Ω for chip B—are well within a factor of two of the experimental findings, with no free-fitting parameters.

In a slightly more sophisticated model, we distribute the magnetic charge evenly within F, up to a distance δ away from the film edge. Magnetic force microscopy performed on edges of similar ferromagnetic films shows gradients, presumably due to closure domain structure, that decay on the scale of a few hundred nm. Roughness due to liftoff was also observed on this size scale. These are modeled by varying δ between 0.5 and 1.5 μm. Using this rectangular volume of magnetic charge, we calculate $B_\perp(r)$, and thereby ΔR_H, as a

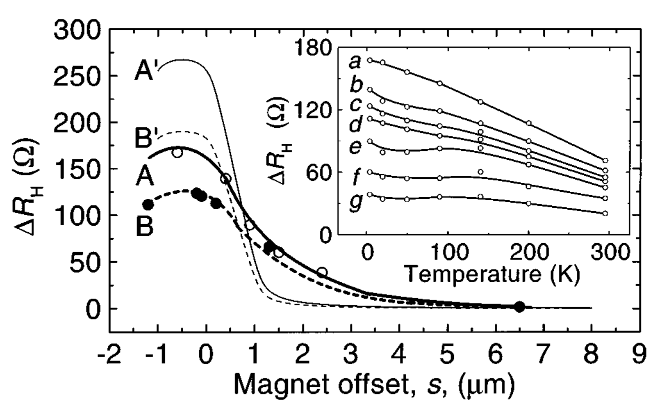

FIG. 3. Comparison between experimental (curves A and B) and theoretical (curves A' and B') ΔR_H, vs s, for both chips. Chip B curves are dashed. The films on chip A were 50% thicker than those on B. *Inset*: temperature dependence of ΔR_H for devices with different values of s: (a) $s=-0.6$, (b) 0.4, (c) -1.2, (d) -0.2, (e) 0.9, (f) 1.5, and (g) 2.4 μm. Curves (c) and (d) are from chip B devices, the rest from chip A. A negative value for s indicates a film F that overlapped the center of the cross junction, whereas a positive value indicates a film F that was stepped back from the junction center.

function of the separation s. Results for $\delta=1\ \mu$m are displayed as solid (A') and dashed (B') traces in Fig. 3 for chips A and B, where the value of n_s measured at $T=4.2$ K is employed. The fact that values of ΔR_H are still found to decay more quickly with s than shown by experiment suggests a more detailed treatment of the local field profile is required.

The temperature dependence of ΔR_H, displayed in the inset of Fig. 3, does not stem from the magnetic properties of F. Our separate measurements of $\mathbf{M}$ in larger, but otherwise identical, films confirmed that M_s was not temperature sensitive; it decreased by at most a few percent from $T=4.2$ to $T=300$ K. Instead, an increase of n_s with increasing temperature (Fig. 4) gives rise to a corresponding decrease in ΔR_H. To analyze this further, we plot the apparent average field that generates R_H, $\langle B_\perp \rangle_{\text{eff}}=\Delta R_H n_s e$, deduced using measured values of ΔR_H and n_s, in the inset of Fig. 4. The lower traces, (e)–(g), show very little temperature dependence, confirming that the dependence of R_H on n_s largely accounts for the temperature variation of ΔR_H. In traces (a)–(d), obtained for devices with small separations s, however, $\langle B_\perp \rangle_{\text{eff}}$ is seen to rise at low temperatures. We attribute this to a ballistic enhancement[8] of ΔR_H, at the higher values of $\langle B_\perp \rangle_{\text{eff}}$ associated with small s. This phenomenon occurs from $B_\perp=0$ upward to several times a characteristic field, $B_0=p_F/ew$,[9] in microjunctions where the transport mean free path, $\ell_0=p_F\mu/e$, exceeds their spatial extent, i.e., $\ell_0/w=\mu B_0 \gg 1$. Here $p_F=\hbar(2\pi n_s)^{1/2}$ is the Fermi momentum in 2D. For a given value of $B_\perp$, the net effect is to enhance R_H, and with it the apparent value of $\langle B_\perp \rangle_{\text{eff}}$ above that of the actual field acting upon the microjunction. In the inset of Fig. 4, we plot two contours, for $\ell_0/w=\mu(T)\times\langle B_\perp \rangle_{\text{app}}=0.1$ and 1.0, using $\mu(T)$ as measured. These roughly demarcate the regimes where ballistic enhancement first sets in, then becomes fully developed.

To summarize, the new potential of these hybrid devices lies in the fact that the Hall resistance, $R_H(\langle B_\perp \rangle_{\text{eff}})$, can be much greater than that obtained in standard Hall devices (i.e., without ferromagnets) subjected to a perpendicular field of the same magnitude as our parallel fields. In effect, these devices provide a magnetic field ''multiplication.'' In the initial experiments described here, this multiplication is quite modest. At $T=300$ K, the maximum Hall resistance obtained in our hybrid devices at $R_H(H_\parallel \sim 100\ \text{Oe}) \sim 35\ \Omega$, whereas in a standard device with comparable perpendicular field $R_H(100\ \text{Oe}) \sim 27\ \Omega$, hence a multiplication ratio of ~ 1.3 is obtained. There are two principal ways in which this ratio can be greatly enhanced in optimized devices: (i) in high quality, low coercivity ferromagnetic films switching can occur for $H_\parallel \sim 10$ Oe, immediately raising this ratio by an order of magnitude, (ii) careful engineering of the junction geometry and the use of shallow 2DEGs will permit efficient sensing of $B_\perp(\mathbf{r})$ without averaging over low field regions—it is reasonable to expect that $\langle B_\perp \rangle$ of order a tenth the saturation magnetization of the film (here $M_s \sim 1.05$ T) should be achievable. This would yield another order of magnitude improvement.

In this letter, we have described a simple device that takes advantage of the large, easily switched, local field at the edge of a single μm-scale ferromagnetic film. The low coercive fields found in our devices extend the possibility of nonvolatile memory elements employing device-integrated write wires fabricated over the ferromagnetic films. With manipulation of the easy-axis direction of magnetization in the ferromagnetic films, applications such as magnetic field sensors can also be envisioned. Our results indicate that local Hall devices should be realizable using a wide variety of ferromagnetic and semiconductor materials. Finally, since the fringe fields are maximal over a length scale of order 100 nm, we expect that the performance of these devices will actually improve as their size scale is reduced. We are currently exploring these prospects.

The authors thank A. N. Cleland for valuable suggestions in the course of both fabrication and measurement. We gratefully acknowledge support from the ONR under Grant Nos. N00014-96-1-0865 and N00014-96-WX21047, and from the Army NDSEG Fellowship Program.

[1] For a recent review, see G. A. Prinz, Phys. Today **48**, 58 (1995).
[2] M. A. M. Gijs, S. K. J. Lenczowski, and J. B. Giesbers, Phys. Rev. Lett. **70**, 3343 (1993).
[3] J. S. Moodera, L. R. Kinder, T. M. Wong, and R. Meservey, Phys. Rev. Lett. **74**, 3273 (1995).
[4] M. Johnson, Phys. Rev. Lett. **70**, 2142 (1993).
[5] Other simple devices which also rely on an in-plane film magnetization are discussed by G. A. Prinz, Science **250**, 1092 (1990).
[6] We use a value of permalloy measured on a test strip deposited under identical conditions as the sample films. Thermal evaporation yields a slightly Ni-poor film. See K. R. Carson and M. L. Rudee, J. Vac. Sci. Technol. **7**, 573 (1970).
[7] We account for the undercut of the mesa etch, ~ 0.1–$0.2\ \mu$m, and depletion at the channel edges, $\sim 0.3\ \mu$m, leaving an electrical channel width of about $2.2\ \mu$m. See K. K. Choi, D. C. Tsui, and A. Alavi, Appl. Phys. Lett. **50**, 110 (1987).
[8] M. L. Roukes, A. Scherer, S. J. Allen, H. G. Craighead, R. M. Ruthen, E. D. Beebe, and J. P. Harbison, Phys. Rev. Lett. **59**, 3011 (1987).
[9] C. W. J. Beenakker and H. van Houten, Phys. Rev. Lett. **63**, 1857 (1989).
[10] Our structures are not optimized from a device standpoint. The room temperature 2DEG sheet resistance is $R_\square=3.2\ \text{k}\Omega$. In a compact cross junction, the minimum *longitudinal* resistance attainable involves roughly ~ 3 squares, this would yield a $R_{\text{series}} \sim 10\ \text{k}\Omega$. Given our $\Delta R_H \approx 70\ \Omega$, to obtain an appreciable Hall (i.e., *transverse*) output voltage swing of ≈ 20 mV requires $I \approx 300\ \mu$A. For a local Hall element, this would result in power dissipation during read cycles of order 1 mW (longitudinal voltage drop ~ 3 V). The lead resistances arising from long paths in our initial chip layout required use of smaller source currents ($\leq 1\ \mu$A) and, hence, produced smaller output voltages.